IEEE Access
Multidisciplinary | Rapid Review | Open Access Journal

Received August 30, 2020, accepted September 25, 2020, date of publication September 29, 2020, date of current version October 30, 2020.

Digital Object Identifier 10.1109/ACCESS.2020.3027737

Information Transmission Schemes Based on Adaptive Coded Modulation for UAV Surveillance Systems With Satellite Relays

RUI XUE[1], MINGFEI ZHAO[1], AND HUAIYU TANG[2]
[1]College of Information and Communication Engineering, Harbin Engineering University, Harbin 150001, China
[2]China Research Institute of Radiowave Propagation, Xinxiang 453000, China

Corresponding author: Mingfei Zhao (zhaomingfei0825@hotmail.com)

This work was supported in part by the National Natural Science Foundation of China under Grant 61873070, in part by the Technology Development Project of the China Research Institute of Radiowave Propagation under Grant JW2019-114, in part by the Heilongjiang Provincial Natural Science Foundation of China under Grant LH2020F018, and in part by the Heilongjiang Province Key Laboratory of High Accuracy Satellite Navigation and Marine Application Laboratory under Grant HKL-2020-Y03.

ABSTRACT To expand their search range, unmanned aerial vehicles (UAVs) used for surveillance employ satellites as relays to forward monitoring data to the UAV's command and control centers. With updated sensors, the amount of UAV detection data increases sharply, and the demand for bandwidth and transmission rates increase continuously. In this paper, the Ka-band is introduced to the satellite system as a solution instead of the Ku, C and other bands. Highly robust constant coded modulations (CCMs), such as the binary low-density parity-check (LDPC) and the coded quadrature phase shift keying (QPSK) are adopted to handle poor channel conditions caused by rain attenuation, which lead to a waste of spectral efficiency, especially in poor weather conditions; Adaptive Coded Modulation (ACM) can relieve the problems detailed above. Aiming at the problem mentioned above, we have proposed two different transmission schemes for two typical scenarios, including high quality of service (QoS) and high throughput service. The first is the so called automatic repeat request (ARQ)+ACM (target bit error rate (BER) algorithm) for high QoS, which means ARQ and ACM are employed by UAV-satellite links and satellite-center links, respectively. The second, denoted as coded cooperation (CC)+ACM (the maximum throughput algorithm) for high throughput services, designates that CC is employed for UAV-satellite links and ACM is employed for satellite-center links. Simulation results show that the ARQ+ACM scheme achieves higher spectral efficiency than CCM in cases that keep the BER below 10^{-5}, and the CC+ACM scheme attains 3 to 7.5 times the spectral efficiency of CCM.

INDEX TERMS ACM, ARQ, CC, UAV.

I. INTRODUCTION

Recently, wireless communications aided by unmanned aerial vehicles (UAVs, also known as drones) are receiving increased attention from the academic and industrial fields as well as from the military and civilian applications [1]–[4]. This accomplishes a reduction in drone manufacturing costs [2]. Due to their ease of deployment, low cost, high mobility and ability to hover [5], [6] compared to conventional terrestrial infrastructure, UAVs are better equipped to set up wireless links with favorable channel conditions. They are considered a promising vector of support for wireless communications for a great number of practical applications, such as security and surveillance, the real-time monitoring of road traffic, provision of wireless coverage, sensor data collection, relays for ad hoc net-works [3], search and rescue operations, the delivery of goods, data rate enhancement [4], precision agriculture, and civil infrastructure inspection [7], as shown in Figure 1. However, it is difficult to complete complex surveillance missions in remote areas because of the intricate and uncertain circumstances that restrict the ability of UAV to work over larger areas. The solution to this problem is to use satellite relays to transmit the surveillance data.

The associate editor coordinating the review of this manuscript and approving it for publication was Zeeshan Kaleem.

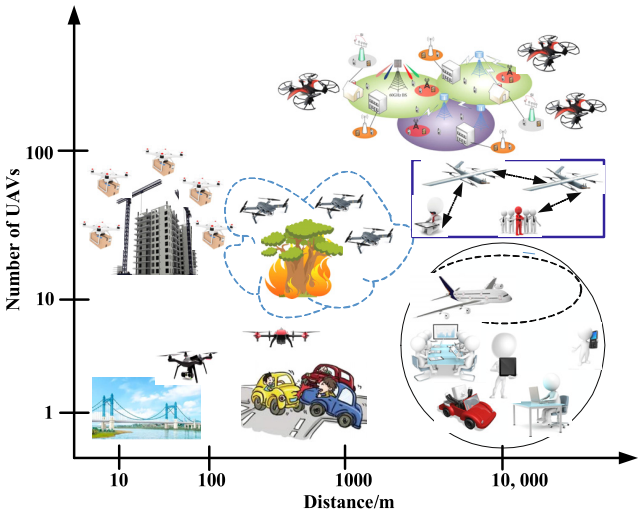

FIGURE 1. Application areas of UAV.

Communication interruptions are inevitable for long-distance transmissions or for physical obstructions but real-time transmissions are guaranteed by satellite relays. Transmissions of surveillance data by UAVs via satellite relays not only ensures the timeliness of the information but also further expands the surveillance range of the UAV. The idea of using relays for communications have been discussed since the work of Cover and El Gamal [8], but not until the work of Sendonaris *et al.* [9] was a cooperative communication scheme and system description formulated in detail. The basic principle of cooperative communications is the use of complimentary communication devices to relay transmissions [10]. A communications system with a satellite relay has natural advantages for telemetry, tracking, commands and supporting communications [11].

Amplify and forward (AF), decode and forward (DF) and coded cooperation (CC) are the main functions in a cooperative relay system, and as a product of channel coding and cooperation techniques, CC has obvious advantages compared to AF and DF. Because of the error bits that are used in relay decoding, it is unreasonable to expect the results of relay decoding to be accurate when there is an uncertain channel environment in the cooperative coding system [12]. As there is a strong demand for QoS for vital information transmissions, this paper adopts an ARQ system with a cyclic redundancy code (CRC) to handle the noise in the UAV-satellite channels. CRC is applied for error detection in the satellite relay, as it is efficient and convenient and ensures the correctness of the relay decoding in the channel in the presence of noise [13]–[18].

With updated sensors, UAVs have faster sensing capabilities and can process information more efficiently; in addition, the quantity of UAV detection data expands rapidly, and the demand for bandwidth and the transmission rate increases apace. The increased demand for satellite communication channel capacity and the crowded operations of the C-band (6/4 GHz), X-band (8/7 GHz), and Ku-band (14/12 GHz), means higher bands and a larger bandwidth satellite communication system is required. The use of Ka-band (30/20 GHz) satellite communications has become a predictable trend in satellite communications because of its high bandwidth, large capacity, small terminal size and strong anti-jamming capabilities [19]. The Ka-band communication is an important advancement in satellite communications; rain fade has been the main factor that restricts the engineering application [20], and the power loss difference resulting from the weather can exceed 20 dB. The signal transmission schemes in the Ka-band communication links primarily employ CCM to resist the rain attenuation or bad channel conditions, which leads to a waste of bandwidth. To improve the spectral efficiency over Ka-band channels, ACM schemes have been recently applied to Ka satellites.

As shown in Figure 1, transmission requirements differ for various scenarios. CCM with high robustness was selected in previous schemes to resist rain attenuation, which guarantees the validity of transmission. However, the previous scheme has resulted in a waste of spectrum resources. The proposed scheme can adapt to the transmission requirements in different scenarios. In addition, applying ACM to satellite relay can improve spectral efficiency and power efficiency of the system. For instance, applications such as traffic monitoring and civil infrastructure inspections require specific quality of services (QoS), such as precise locations. The ARQ+ACM scheme provides high QoS to meet the demand in these cases. Urgent information generated in surveillance missions, such as forest fire warnings, require high throughput. The CC+ACM scheme provides high transmission efficiencies to guarantee the real-time performance. The scheme proposed in this paper will not only improve the spectral efficiency of the UAV system, but also make the UAV surveillance system more flexible and adaptive to the different scenarios. The choice of different transmission mechanisms for various requirements makes the UAV very efficient for surveillance.

The rest of the paper is organized as follows: Section II establishes the system model, including working process for two schemes, channel model of Ka-band and M_2M_4 for SNR estimators. Section III presents the transmission mechanism of the ACM scheme based on CC. The transmission mechanism of the ACM scheme based on ARQ is proposed in Section IV. Simulation results are discussed in Section V. Finally, we provide concluding remarks Section VI.

II. SYSTEM MODEL

To enlarge the coverage area, a UAV dispatched for surveillance missions has to employ satellites as relays to transmit messages. As shown in Figure 2, a conventional structure of the UAV system consists of a surveillance drone, a satellite relay, as well as a destination node. Traditional satellite relays send the received information directly to the command and control center when the distances are beyond the communication range; typically, this is for the purpose of expanding the surveillance range or because obstacles are present. However, different transmission requirements are generated when different information is sent back. In this paper, two

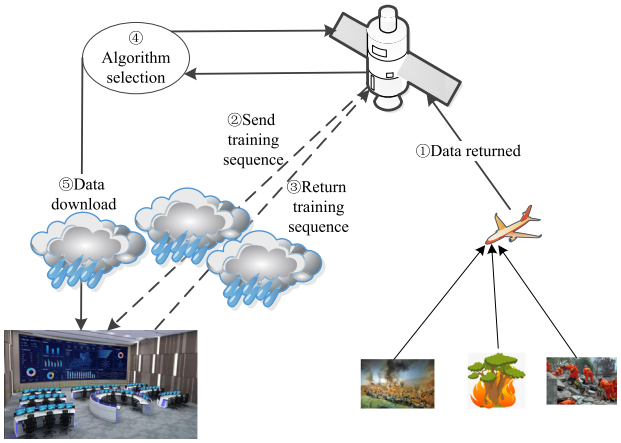

FIGURE 2. The ARQ+ACM scheme.

different transmission schemes are designed according to two typical requirements, CC+ACM and ARQ+ACM. Both transmission schemes have consisted of SNR estimation and Ka-band channel model. Therefore, we introduce the system model from three aspects, including working process for two schemes, channel model of Ka-band and M_2M_4 for SNR estimators.

A. WORKING PROCESS FOR TWO SCHEMES

When performing surveillance missions, UAVs will obtain various types of surveillance information based on the type of monitoring mission. As shown in Figure 2, urgent tasks and emergencies such as forest fire warnings, earthquake rescues and security and surveillance mean the UAV must transmit the surveillance information apace because of the high timeliness requirement of the system. For example, in an earthquake rescue, the rescue team needs to obtain the scene images and videos to create a rescue plan as soon as possible; in these cases, the information timeliness of the systems has the highest priority. The combination of CC and ACM effectively utilizes the bandwidth advantages of the Ka-band and improves the spectrum efficiency and bandwidth utilization of the system. This transmission mechanism can guarantee the efficient return of important and time-sensitive information in long-distance communications. As shown in Figure 2, the transmission process is as follows:

(1) The UAV sends data back to the satellite.

(2) The satellite sends a training sequence to the command and control center.

(3) The command and control center returns the training sequence back to the satellite. The satellite uses the received training sequence for an SNR estimation and determines the channel's state. Different SNR values can be obtained for different weather conditions.

(4) The satellite selects the target ber algorithm to transmit the information.

(5) Data are downloaded.

When on routine missions, such as the real-time monitoring of road traffic and civil infrastructure inspections, drones opt for a different transmission system, the ACM scheme based on ARQ. The reliability of information obtained by conventional surveillance missions is extremely important. For example, accurate locations and pictures of the scene are very helpful in dealing with accidents when the drones do real-time monitoring for road traffic missions. In these cases, the reliability of the information becomes very important. The transmission system, based on ARQ, can significantly improve the reliability of the system because it guarantees the accuracy of the relay decoding. The system sacrifices some of its timeliness in exchange for more accurate information to meet the needs of conventional UAV surveillance missions. As shown in Figure 3, the working steps of the ARQ+CRC scheme are as follows:

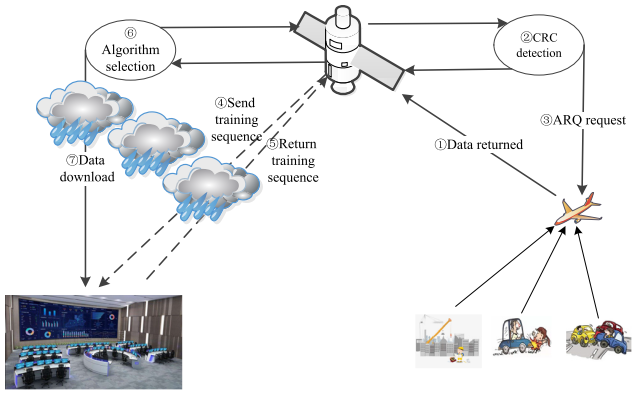

FIGURE 3. The CC+ACM scheme.

(1) The UAV sends data back to the satellite.

(2) The satellite relay will demodulate and decode the information after receiving the data and the CRC is performed simultaneously to judge whether the information decoding is right or wrong.

(3) If there is no error, the system goes to the next step; otherwise, the satellite sends a command for ARQ.

(4) The satellite sends a training sequence to the command and control center.

(5) The command and control center returns the training sequence back to the satellite for SNR estimation.

(6) The satellite selects the maximum throughput algorithm to transmit the information.

(7) Data are downloaded.

As shown above, the process of information of two transmission schemes are introduced. Both transport schemes require the channel model of the Ka-band and the SNR estimators. When transmitted from the satellite to the command and control center, the information goes through Ka-band channel. Therefore, channel model of the Ka-band will be introduced in the following part.

B. CHANNEL MODEL OF THE Ka-BAND

Many factors in the atmosphere, such as precipitation, water vapor, clouds, oxygen, and flickers, cause signal declines in the Ka-band satellite communications. The rain attenuation, which is connected with frequency, weather conditions, and

system availability, is the most important element [21]. These factors can be considered in the satellite communication link by modifying the free space propagation formula. The most serious attenuation of the satellite communication in the Ka-band is the signal attenuation caused by rain decline. As shown in measured data, rain attenuation is a function of system feasibility and carrier frequency. In the case of a large elevations [22], L_r which means rain attenuation can be expressed as

$$L_r = C_1 \exp(\delta_1 f) + C_2 \exp(\delta_2 f) - (C_1 + C_2)\,(\mathrm{dB}), \quad (1)$$

where C_1, C_2, δ_1, and δ_2 are the functions of the system availability, and f is the carrier frequency. When the elevation is small, the formula can be simplified as

$$L_r(\theta) = L_r(\theta_0) \sin\theta / \sin\theta_0\ (\mathrm{dB}), \quad (2)$$

where θ is the elevation of the earth station, and θ_0 is the reference elevation.

When a digital modulation signal represented as $s(t) = \mathrm{Re}[s_1(t)\exp(j2\pi f_c t)]$ is transmitted through the channel, $s_1(t)$ is the time domain complex baseband, and $s_1(f)$ is the frequency domain complex baseband. The equivalent lowpass signal (excluding AWGN) can be expressed as

$$r(t) = \int_{-\infty}^{\infty} C(f,t) s_1(f) \exp(j2\pi f t)\mathrm{d}f, \quad (3)$$

where $C(f,t)$, the time-frequency transfer function can be considered as a complex value independent frequency in the signal bandwidth since the Ka-band fading channel is a nonfrequency selective channel. In view of the spectrum of $s_1(f)$ focused in the adjacent area of $f = 0$ Hz, $C(f,t) = C(0,t)$ can be replaced with Equation (3)

$$\begin{aligned} r(t) &= \int_{-\infty}^{\infty} C(0,t) s_1(f) \exp(j2\pi f t)\mathrm{d}f \\ &= C(0,t) \int_{-\infty}^{\infty} s_1(f) \exp(j2\pi f t)\mathrm{d}f \\ &= C(0,t) s_1(t) \\ &= \alpha(t) \exp(j\theta(t)) s_1(t), \end{aligned} \quad (4)$$

As multiplicative interference has the characteristics of slow time-varying, we can regard the fading characteristics as a constant in a symbol interval. Equation (4) can be simplified as

$$r(t) = \alpha \exp(j\theta) \cdot s_1(t) \quad 0 \le t \le T, \quad (5)$$

where T is the cycle of the modulation symbol, α and θ are the envelope and phase of the equivalent lowpass channel, respectively. The weather conditions are the primary factor affecting satellite communications in the Ka-band as shown in the research. The envelope and phase obey the Gaussian distribution [23], [24], and the probability density function can be expressed as

$$p(\alpha) = \frac{1}{\sqrt{2\pi}\sigma_1} \exp\left(-\frac{(\alpha - m_1)^2}{2\sigma_1^2}\right), \quad (6)$$

$$p(\theta) = \frac{1}{\sqrt{2\pi}\sigma_2} \exp\left(-\frac{(\theta - m_2)^2}{2\sigma_2^2}\right). \quad (7)$$

where, σ_1, σ_2, m_1, and m_2 are available in TABLE 1.

TABLE 1 shows the probability distribution parameters of the signal envelope and the phases for various weather conditions in the Ka-band satellite communication channels [24]. Here, σ_1 and σ_2 are the variances of the signal envelope and phase, respectively, m_1 and m_2 are the mean of the signal envelope and phase, respectively. A considerable number of data from numerous propagation characteristic measurement experiments have been accumulated in previous studies in Olympus-star, Italsat-star and ACTS-star [24], the values are obtained in TABLE 1.

TABLE 1. Ka-band satellite channel envelope and phase model.

Weather conditions	m_1	σ_1^2	m_2	σ_2^2
Clear/cloudy	0.455	0.00056	0.0079	0.00381
Cumulus cloud	0.346	0.00272	0.0154	0.00864
Light rain	0.483	0.00003	0.0088	0.00546
Thunder shower	0.436	0.01386	0.0068	0.00414
Blowing snow	0.500	0.00021	0.0089	0.00435
Ice pellets	0.482	0.00062	0.0094	0.00544
Rain	0.662	0.02000	−0.0089	0.03077

From the analysis above, the channel model of the Ka-band satellite communications can be established as shown in Figure 4. The digital modulation signal can be expressed as a combination of the frequency independent complex multiplicative interference factor and the additive white Gaussian noise (AWGN) after the nonfrequency selective fading channel.

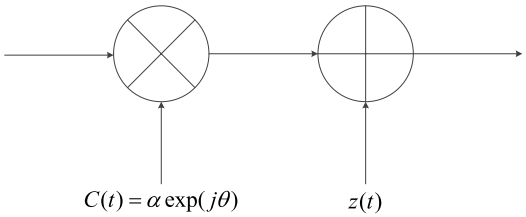

FIGURE 4. Ka-band satellite channel statistical model.

Applying ACM to Ka-band can improve the spectral efficiency of the system. SNR estimation plays an important role in ACM. Above all, the accuracy of SNR estimation is of great significance for ACM scheme selection. M_2M_4 is selected in this paper for SNR estimators, which will be introduced in next part.

C. M_2M_4 FOR SNR ESTIMATORS

It is necessary to estimate the channel state before choosing the transmission scheme. The results of an SNR estimation are very important as the result will be directly used to select the scheme. The performance of the system will be affected when the estimation of SNR differs greatly from

the actual channel state. If the estimated value of SNR is greater than the actual value, the selected scheme cannot guarantee the reliability of the system; otherwise, the system, theoretically, cannot reach the maximum transmission rate. Therefore, an accurate SNR estimation method is the key factor affecting the system performance.

The SNR estimation method consists of time domain and frequency domain methods. The time domain method can be divided into data-aided (DA) and non-data aided (NDA) methods [25]. The DA method has higher estimation accuracy than the NDA method but involves the insertion of a periodic pilot sequence, which is inefficient. Common methods of SNR estimations are DA ML and M_2M_4. The DA ML estimator requires the receiver and prior information sequences of the transmitter. However, obtaining prior information is impossible in some practical application cases. This paper adopts the M_2M_4 estimation method without a prior information sequence. After sampling the received signal, the output sequence is expressed as

$$r_k = A_{Sk} + z_k \quad k = 1, 2, \cdots, K \tag{8}$$

where K is the observation point after sampling, r_k obeys the Gaussian distribution, A_{Sk} is the mean, and δ^2 is the variance.

The two-order moments and four-order moments of the received sequence in Equation (8) can be expressed as

$$M_2 = E[r_k r_k^*] = A^2 E[|s_k|^2] + AE[s_k z_k^*] + AE[s_k^* z_k] + E[|z_k|^2], \tag{9}$$

and

$$\begin{aligned} M_4 &= E[(r_k r_k^*)^2] \\ &= A^4 E[|s_k|^4] + 2A^3(E[|s_k|^2 s_k z_k^*] + E[|s_k|^2 s_k^* z_k]) \\ &\quad + A^2(E[(s_k z_k^*)^2] + 4E[|s_k|^2 |z_k|^2] + E[(s_k^* z_k)^2]) \\ &\quad + 2A(E[|s_k|^2 s_k z_k^*] + E[|z_k|^2 s_k^* z_k]) + E[|z_k|^4] \end{aligned} \tag{10}$$

where the conjugate of r_k, s_k and z_k are denoted r_k^*, s_k^* and z_k^*, M_2 and M_4 are the two-order moments and four-order moments respectively.

Considering that the signal and noise are independent of one another, and the mean is zero, Equations (9) and (10) can be simplified as follows

$$M_2 = A^2 + \delta^2, \tag{11}$$

and

$$M_4 = A^4 + 4A^2\delta^2 + 2\delta^4, \tag{12}$$

the estimated value of A and δ^2 can be expressed as

$$\hat{A}_{MM}^2 = \sqrt{2(M_2)^2 - M_4}, \tag{13}$$

and

$$\hat{\delta}_{MM}^2 = M_2 - \hat{A}_{MM}^2, \tag{14}$$

the corresponding SNR estimator is

$$SNR = 10\log_{10}\left(\frac{\hat{A}_{MM}^2}{m_1^2 \hat{\delta}_{MM}^2}\right), \tag{15}$$

M_2 and M_4 can be received in practical applications through the receiving sequence average value and expressed respectively as

$$M_2 = \frac{1}{K}\sum_{k=1}^{K} |r_k|^2, \tag{16}$$

and

$$M_4 = \frac{1}{K}\sum_{k=1}^{K} |r_k|^4. \tag{17}$$

The estimation of the M_2M_4 performs better with the higher number of observation points. When the SNR is high, the M_2M_4 estimators have a similar estimation performance to DA ML, and the observation points have no influence on the estimation performance [26]. Increasing the number of sampling points per symbol and the length of the information sequence sent are effective means to achieve better performance estimations when the channel environment is poor in the application of the actual Ka-band channel. The M_2M_4 estimators have a better estimation performance and can be approximated as unbiased in the commonly used SNR range.

III. THE CC+ACM SCHEME FOR HIGH THROUGHPUT

Besides channel model of Ka-band and M_2M_4 for SNR estimators, the coded cooperation system and maximum throughput algorithm are also important parts for this scheme. The CC+ACM scheme aims at high throughput, which is different from the ARQ+ACM scheme. One of the features of the transmission system is that the relay no longer directly forwards information, instead the information in the UAV-satellite data link is decoded and forwarded. After that, the satellite downloads the data through ACM for maximum throughput algorithm to combat the effects of weather changes in the Ka-band communication. For the relay, its work includes decoding, signal noise ratio (SNR) estimation and the selection of a suitable ACM scheme for encoding and modulation to send information. Although the relay cannot guarantee that the decoding has no errors, some of the noise effects of the UAV-satellite channel can be eliminated in this way. The flow chart of the UAV-satellite-command and control center communication link is shown in Figure 5. Coded cooperation system ensures that the scheme with the maximum throughput is selected. We will introduce the coded cooperation system in next part.

A. CODED COOPERATION SYSTEM

The satellite relay is the most important part of the whole communication link. In a coded cooperation system, the satellite decodes and recodes the information instead of directly forwarding the information. CC combines efficient channel coding technology with collaboration technology to improve the performance of the communication system. In addition to improving BER performance, there are many extra advantages to applying CC to relay information as enumerated as follows:

(1) From a power point of view, the performance gain increases by CC can be redirected to reduce the sending power of the nodes and reduce the interference between users.

(2) Relay collaboration can extend the coverage of existing structures such as cellular networks and reduce the blind areas in communications.

(3) Most importantly, the relay cooperation can reduce the sensitivity to channel changes, thereby decreasing the interruption probability for real-time services (such as voice, video, etc.) and providing better QoS.

Based on the characteristics of CC, the process of decoding and recoding of the information can be combined with ACM, which means that the satellite selects the most efficient coded modulation scheme (CMS) to transmit information. The ACM selection will be introduced in the next section.

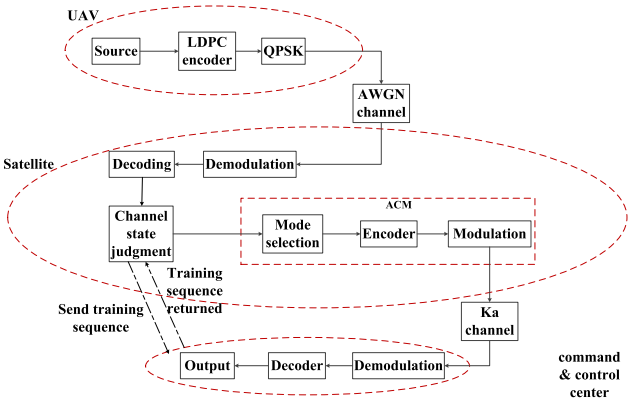

FIGURE 5. System model of the scheme based on CC.

B. MAXIMUM THROUGHPUT ALGORITHM OF ACM

As shown in Figure 5, we select the ACM scheme according to the results of SNR estimations [27]. As mentioned above, the satellite downloads data through the Ka-band channel, which is obviously affected by the rain decline. To guarantee the performance of the satellite system in bad weather, the satellite incorporates large error margins, which leads to a waste of power in better weather conditions. Due to the high bandwidth of the Ka-band, in order to avoid the power waste caused by the large rainfall reserve of the relay, the satellite downloads data by ACM. Next, we will introduce the ACM selection on the Ka-band.

In the cooperative relay system, it is necessary to select a suitable scheme according to the channel status. Assuming the transmission loss approximates to the rain attenuation, which is related to the frequency, weather conditions and system availability, we can estimate the SNR at the receiving end.

The scheme switching strategy is shown in Figure 6, where E_b/N_0 is the SNR estimation by M_2M_4. A, B, C, D are a set of threshold values, satisfying the condition of $A < B < C < D$, CMS 1∼CMS 5 are five alternative schemes, with an increasing spectrum utilization. There are five intervals according to the threshold values $(0, A]$, $(A, B]$, $(B, C]$, $(C, D]$ and $(D, \infty]$, one for each alternative scheme.

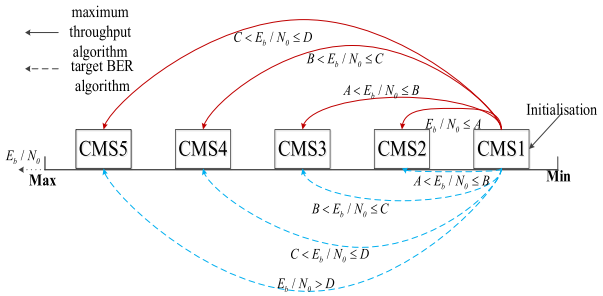

FIGURE 6. Schemes switching strategy.

In this paper, we used QPSK, 8 phase shift keying (8PSK), 16 amplitude phase shift keying (16APSK), 32 amplitude phase shift keying (32APSK) modulations, and LDPC is adopted as the channel coding according to the digital video broadcasting - satellite - second generation (DVB-S2) [23]. Code rates include 1/4, 1/2, 2/3 and 3/4. The five schemes can be seen in TABLE 2.

TABLE 2. Five schemes.

Scheme	Modulation	Code rate
CMS 1	QPSK	1/4
CMS 2	8PSK	1/2
CMS 3	16APSK	1/2
CMS 4	16APSK	2/3
CMS 5	32APSK	3/4

According to different requirements in different scenarios, this paper designs two ACM scheme selections, the target BER algorithm and the maximum throughput algorithm. As mentioned above, the transmission rate is a critical indicator when transmitting important information. Therefore, we select a maximum throughput algorithm. This algorithm is suitable for services without constraints on the maximum acceptable BER. High transmission efficiency is guaranteed.

BER switching thresholds are derived from the cross-point of CMS throughput curves as shown in Figure 9.

For example, for E_b/N_0 values between 12 dB and 15 dB, the 16APSK modulation scheme with a code rate equal to 1/2 can be utilized, resulting in the maximum throughput. Over this threshold, there are modulations for schemes that provide higher throughput, such as a 16APSK modulation scheme with a code rate equal to 2/3. Figure 9 also shows that 32APSK can be utilized with a code rate of 3/4 when the E_b/N_0 values exceed 17.5dB and results in a spectral efficiency of 3.75bps/Hz. The switching threshold of each scheme is shown in TABLE 3.

Throughput T is defined as follows:

$$T = R(1 - \mathrm{FER}). \tag{18}$$

where R is the rate of information, which is assumed as 1 in this system and the FER is the frame error rate.

TABLE 3. Schemes based on maximum throughput algorithm.

E_b / N_0	CMS
$E_b / N_0 \leq 10.5$	QPSK 1/4
$10.5 < E_b / N_0 \leq 12$	8PSK 1/2
$12 < E_b / N_0 \leq 15$	16APSK 1/2
$15 < E_b / N_0 \leq 17.5$	16APSK 2/3
$E_b / N_0 > 17.5$	32APSK 3/4

IV. THE ARQ+ACM SCHEME FOR HIGH QoS

As mentioned above, the relay decoding is not fully guaranteed to be error-free. In addition, it is unreasonable to consider the satellite relay as an ideal relay. In situations where the accuracy of information is very important, adding ARQ to the relay can effectively improve the accuracy of decoding. To ensure the validity of the relay decoding, CRC is added to the UAV data chain, in which case the system eliminates the influence of the UAV-satellite channel on the information. After this, the satellite downloads the data through ACM for target BER algorithm to combat the effects of weather changes in the Ka-band communication. The flow chart of the UAV-satellite-command and control center communication link is shown in Figure 7. The data transmission goes through the Gaussian channel of the UAV-satellite link and the Ka-band channel of the satellite-command and control center link.

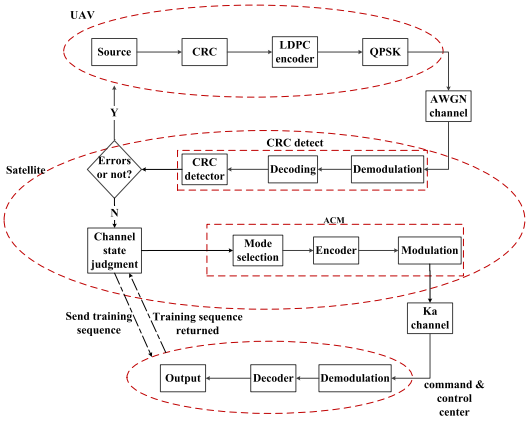

FIGURE 7. System model of the scheme of ACM based on ARQ.

For example, when the UAV is involved in real-time monitoring of road traffic missions, details such as the location and the scene of the accident are very important. The relay can fully recover the original information of the UAV for the transmission system, in this way the noise impact of the UAV-satellite channel is completely eliminated. The relay determines whether to execute ARQ by determining if there is an error. The CRC detection and ACM selection are introduced in the following section.

A. CRC DETECTION

CRC is added to UAV surveillance information before encoding and modulation to make preparations for the relay to judge whether the decoding is correct. It is necessary for the satellite relay to decode information correctly, which can improve the performance of the UAV-satellite- command & control center system. In this paper, CRC is added on the basis of UAV data link, which can effectively determine whether the relay decoding is correct. When the decoding is correct, the satellite relays the information to the command & control center; otherwise, a command is sent for ARQ.

As mentioned above, the CRC is generated by several special polynomials, which commonly include CRC 12, CRC 16 and CRC 24. Different checksums lead to different performances. In general, CRC 24 performs better than CRC 16 and CRC 16 performs better than CRC 12. In practical applications, different checksums are selected according to different requirements. As CRC 12 has poor performance and CRC 24 has a high complexity, this paper selects CRC 16 to encode the information from UAV.

All the code polynomial $T(x)$ of a CRC can be divided by the generator polynomial $g(x)$ as a CRC has all the characteristics of the quasi-cyclic code. We set $m(x)$ the information code polynomial, $(k-1)$ the highest time. k is the number of information codes. We obtain $x^{n-k} \cdot m(x)$ by multiplying x^{n-k} times $m(x)$. Dividing $x^{n-k} \cdot m(x)$ by $g(x)$ can conclude:

$$\frac{x^{n-k} \cdot m(x)}{g(x)} = Q(x) + \frac{r(x)}{g(x)}, \tag{19}$$

where the remainder $r(x)$ is appended to the information code polynomial as a check-code polynomial, we obtain a code polynomial:

$$T(x) = x^{n-k} \cdot m(x) + r(x), \tag{20}$$

the polynomial of CRC 16 we use in this paper can be expressed as:

$$g(x) = x^{15} + x^{14} + x^2 + 1, \tag{21}$$

$R(x)$ is the received code set polynomial in the CRC detection. The relay determines whether there are errors in the remainder of receiving code by calculating whether the result is zero. $E(x)$ is the error code in the receiving signals, the receiving code polynomial satisfies:

$$\frac{R(x)}{g(x)} = \frac{T(x) + E(x)}{g(x)}. \tag{22}$$

If no error occurred in transmissions, the receiving code will be the same as the transmitting code $R(x) = T(x)$, and $R(x)$ must be divisible by $g(x)$, in which condition the data can be transmitted to the next section; otherwise, the system will send a command to the ARQ. In order to ensure the reliability of the system, we select target BER algorithm of ACM, which keeps the BER below a certain value all the time.

B. TARGET BER ALGORITHM OF ACM

After the information obtained by the relay decoding is proved to be correct by the CRC, the relay can recode and modulate the original information. As mentioned above, the satellite downloads data through the Ka-band channel, which

is obviously affected by the rain decline. Due to the high bandwidth of the Ka-band, the satellite downloads data by ACM to avoid the power waste caused by the large rainfall reserve of the relay. The satellite selects the transmission scheme based on the results of the SNR estimation.

The ACM scheme selected in this paper is based on DVB-S2, we choose QPSK, 8PSK, 16APSK, and 32APSK modulations, and LDPC is adopted as the channel coding according to the DVB-S2. Code rates include 1/4, 1/2, 2/3 and 3/4. According to the characteristics of the Ka-band channel, this paper establishes the Ka-band channel model and deduces the channel characteristics in various weather conditions as mentioned above in Section II. The channel state is estimated by an SNR estimation and the data are downloaded according to the current state of the channel.

The target BER algorithm is selected since this system requires more accuracy of information. This algorithm is suitable for a service whose QoS needs to be guaranteed. Given the target BER limit, the E_b/N_0 switching thresholds for the coding and modulation options can be derived. Different target BER limits result in different E_b/N_0 switching thresholds. In this paper, the target BER limit equals to 10^{-5}. Figure 8 shows a comparison of BER performance and the E_b/N_0 values of different schemes.

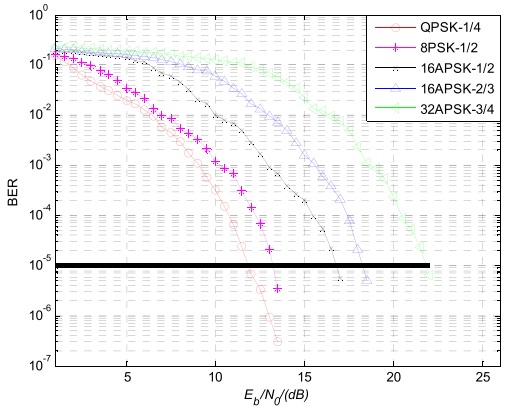

FIGURE 8. BER switching thresholds based on target BER algorithm.

For example, for the E_b/N_0 values below 16.5 dB, the 16APSK modulation scheme with a code rate equal to 1/2 cannot be selected, resulting in a BER higher than 10^{-5}. When higher than this threshold, the CMS confronts the execution criterion. In this case, the spectral efficiency becomes 2bps/Hz. In addition, Figure 8 also shows that 32APSK can be utilized with a code rate of 3/4 when the E_b/N_0 values exceed 22 dB, and the results are in a spectral efficiency of 3.75bps/Hz. The CMS is shown in TABLE 4.

V. NUMERICAL RESULTS AND ANALYSIS

The validity of the proposed CC scheme based on ACM and the ARQ scheme based on the ACM scheme for UAV-satellite-command and control center communications are then tested. Monte Carlo simulations the software are performed to evaluate the performance of the above system compared to the fixed modulation and coding (FMC)

TABLE 4. Schemes based on the target BER algorithm.

E_b / N_0	CMS
$E_b / N_0 < 13$	QPSK 1/4
$13 \le E_b / N_0 < 16.5$	8PSK 1/2
$16.5 \le E_b / N_0 < 18.5$	16APSK 1/2
$18.5 \le E_b / N_0 \le 22$	16APSK 2/3
$E_b / N_0 \ge 22$	32APSK 3/4

(the QPSK modulation scheme with a code rate equal to 1/4). In simulations, uplink data between UAV and satellites passes through a Gaussian white noise channel, and downlink data between the satellite and command and control center passes through a Ka-band channel, which assumes rainy weather depending on the characteristics of the UAV and the satellite. The binary information frame length is 192 bits, and the value of q is taken to 2. The $\mathbf{H}$ with a lower triangular is constructed by a QC algorithm, then the $\mathbf{G}$ is derived through Gaussian elimination [28], [29]. The Log-FFT-BP algorithm is adopted for LDPC decoding. The frame number is set to 100000 and the maximum number of retransmissions for the ARQ system is set to 100. At last, the iteration number of the Log-FFT-BP algorithm is set to 25.

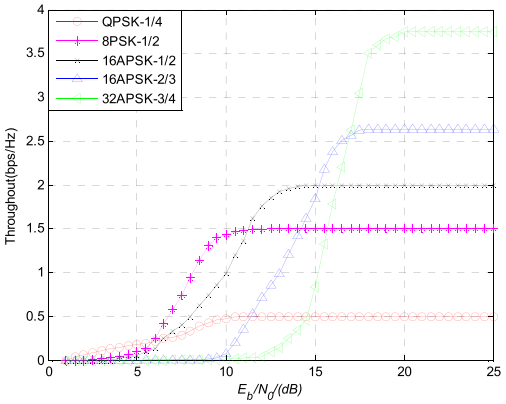

FIGURE 9. Throughput performance of five schemes.

The target BER algorithm is suitable for services where QoS needs to be guaranteed. Therefore, the target BER algorithm is set to the schemes based on ARQ, which requires high QoS. In this paper, the target BER limit is set as 10^{-5}. Figure 8 illustrates the BER performance versus E_b/N_0 for the proposed ACM scheme. We can observe from Figure 8 that all the alternatives for the scheme based on ARQ in the proposed ACM scheme could meet the requirement of the BER limit when E_b/N_0 is in a certain region. To guarantee the uniqueness of scheme switching, the values of E_b/N_0 at BER $= 10^{-5}$ for different candidates do not coincide with each other. Figure 10 shows the BER versus E_b/N_0 for three algorithms, including the target BER algorithm, the maximum throughput algorithm, and the FMC algorithm. The fluctuating point in the figure is the position of the scheme switch.

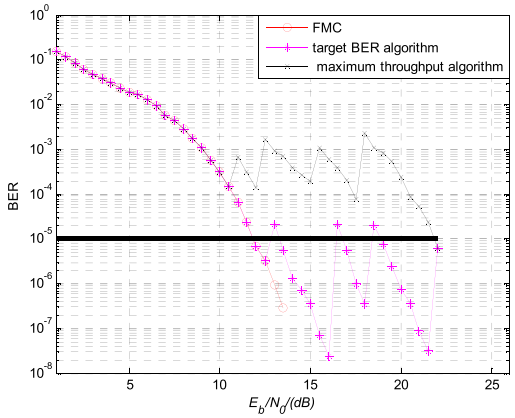

FIGURE 10. BER performance of three schemes.

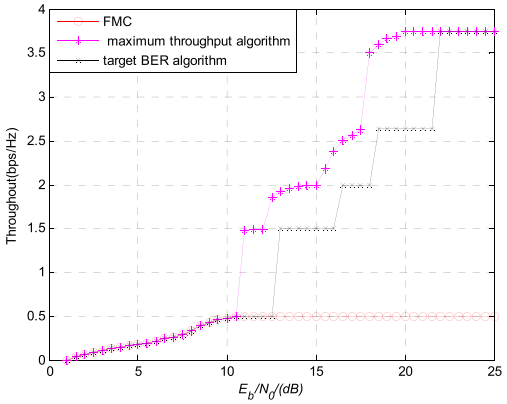

FIGURE 11. Throughput performance of three schemes.

It can be seen that for E_b/N_0 values below 13 dB, the three algorithms produce almost the same value of BER. However, over this threshold, the target BER algorithm gives the best BER value. For instance, for the E_b/N_0 value of 15 dB, the BER of the target BER algorithm is lower than 10^{-7} and the BER of the maximum throughput algorithm is higher than 10^{-4}. For the value of BER is 10^{-5}, the maximum throughput algorithm cannot reach the certain value, and the FMC algorithm and target BER algorithm will keep the value of BER below 10^{-5} when the value of E_b/N_0 is over 13 dB. In addition, Figure 10 also shows that when the values of E_b/N_0 are higher than 13 dB, the target BER algorithm gives a higher spectral efficiency than the FMC algorithm, while keeping the value of BER below 10^{-5}. More details about the CMS are listed in TABLE 3.

The maximum throughput algorithm is suitable for services whose transmission rate needs to be guaranteed. Therefore, the maximum throughput algorithm is set to the CC scheme based on ACM. Figure 9 shows the throughput performance versus E_b/N_0 for the proposed ACM scheme. We can observe from Figure 9 that the maximum throughput of different schemes varies. Figure 9 illustrates the throughput curves versus E_b/N_0 for the three schemes.

It clearly appears that the reference ACM and FMC have the same throughput performance when E_b/N_0 is below 11 dB. Over this threshold, the reference ACM has a better throughput performance than FMC. We also observe from Figure 11 that the candidate in the proposed ACM scheme can obtain a higher spectral efficiency than the target BER algorithm. For instance, when the value of throughput is 3, the FMC algorithm cannot reach this value, and the target BER algorithm reach this value when the value of E_b/N_0 is 22 dB and the maximum throughput algorithm is 17dB, which makes the latter have a gain of 5 dB. Through the above analysis we deduce that the proposed ACM scheme can significantly improve the spectral efficiency with the same transmitting power compared to FMC.

It can be seen that the target BER algorithm keeps the BER below 10^{-5} and the maximum throughput algorithm always achieves the maximum throughput. As a result, the target BER algorithm is more suitable for the scheme based on ARQ, which requires a high QoS. Likewise, the maximum throughput algorithm is compatible with the scheme based on CC. In the actual transmission, selecting the appropriate transmission scheme and the corresponding algorithm can achieve the maximum efficiency for the UAV missions.

VI. CONCLUSION

This paper has chiefly discussed the application of different adaptive coded modulation (ACM) schemes for two typical requirements in UAV surveillance systems. Applications of UAV in different scenarios have different requirements. In the existing UAV surveillance systems, large amounts of data are returned in a single method and it is difficult to meet the varied demands of different information transmissions. Focusing on this issue, a novel ACM scheme with ARQ or CC based on CRC detection and LDPC code is proposed, which satisfies the varied requirements in the different scenarios. In two typical scenarios, two different algorithms have been implemented. The target BER, which is adopted for ARQ+CC aims to keep the error rate under a specified value employs the CMS, which respects the error target while guaranteeing the highest efficiency, and the maximum throughput. CC+ACM, conversely, aims at maximizing the system spectral efficiency without controlling the performance of the error rate. The application of ACM to satellite relay in this paper has not been proposed before. In addition, the schemes mentioned in this paper can be more flexible to adapt to different requirements and perform better than the previous CCM. Theoretical analysis and Monte Carlo simulation results over the Ka-band channels based on software show that, compared to the reference UAV transmission scheme, the proposed ARQ+ACM and CC+ACM algorithms can satisfy different requirements in various scenarios. This increases the flexibility of UAVs and extends their surveillance range but also provides a higher spectral efficiency for the same transmitting power. In addition, equipping different ACM algorithms under different schemes can save large quantities of power resource. For UAV surveillance system, it is of great significance to select the appropriate transmission scheme flexibly in different scenarios. In future works, we will try to apply network coding (NC), continue phase modulation (CPM)

and other technologies to UAV monitoring system to further improve the throughput, spectral efficiency and robustness of the system, which enables the UAV to work in more complex scenarios.

REFERENCES

[1] G. Wang, B.-S. Lee, J. Y. Ahn, and G. Cho, "A UAV-aided cluster head election framework and applying such to security-driven cluster head election schemes: A survey," *Secur. Commun. Netw.*, vol. 2018, pp. 1–17, Jun. 2018.
[2] J. Guo, I. Ahmad, and K. Chang, "Classification, positioning, and tracking of drones by HMM using acoustic circular microphone array beamforming," *EURASIP J. Wireless Commun. Netw.*, vol. 2020, no. 1, p. 9, Dec. 2020.
[3] H. Teng, I. Ahmad, A. Msm, and K. Chang, "3D optimal surveillance trajectory planning for multiple UAVs by using particle swarm optimization with surveillance area priority," *IEEE Access*, vol. 8, pp. 86316–86327, 2020.
[4] M. Z. Anwar, Z. Kaleem, and A. Jamalipour, "Machine learning inspired sound-based amateur drone detection for public safety applications," *IEEE Trans. Veh. Technol.*, vol. 68, no. 3, pp. 2526–2534, Mar. 2019.
[5] K. Miranda, A. Molinaro, and T. Razafindralambo, "A survey on rapidly deployable solutions for post-disaster networks," *IEEE Commun. Mag.*, vol. 54, no. 4, pp. 117–123, Apr. 2016.
[6] Y. Zeng, R. Zhang, and T. J. Lim, "Wireless communications with unmanned aerial vehicles: Opportunities and challenges," *IEEE Commun. Mag.*, vol. 54, no. 5, pp. 36–42, May 2016.
[7] R. Xue, L. Han, and H. Chai, "Complex field network coding for multi-source multi-relay single-destination UAV cooperative surveillance networks," *Sensors*, vol. 20, no. 6, p. 1542, Mar. 2020.
[8] F. Zhang, Y. Zuo, and H. Sun, "Techniques of rain fade countermeasures in ka-band satellite communication on ships," in *Proc. 16th Int. Conf. Opt. Commun. Netw. (ICOCN)*, Aug. 2017, pp. 1–3.
[9] A. Sendonaris, E. Erkip, and B. Aazhang, "User cooperation diversity—Part I: System description," *IEEE Trans. Commun.*, vol. 51, no. 11, pp. 1927–1938, Nov. 2003.
[10] N. Jain, A. Dongariya, and A. Verma, "Comparative study of different types of relay selection scheme for cooperative wireless communication," in *Proc. Int. Conf. Inf., Commun., Instrum. Control (ICICIC)*, Aug. 2017, pp. 1–4.
[11] L. Hui-Min and L. Cheng-Fei, "Technology analysis and scheme design of aerospace vehicles TT&C and communication based on relay satellites," in *Proc. IEEE 9th Int. Conf. Commun. Softw. Netw. (ICCSN)*, May 2017, pp. 794–797.
[12] W. Jin, S. Wu, E. Yang, and J. Jiao, "LDPC convolutional codes coded cooperation based on puncturing," in *Proc. 19th Int. Conf. Adv. Commun. Technol. (ICACT)*, 2017, pp. 505–509.
[13] M. I. Qadri and M. Zia, "Adaptive modulation and coding with selective retransmission under OFDM signaling," *Wireless Pers. Commun.*, vol. 101, no. 4, pp. 1787–1805, Aug. 2018.
[14] K. Kotuliakova, J. Polec, and F. Csoka, "An adaptive ARQ–HARQ method with BCH codes," in *Proc. IEEE 11th Int. Conf. Appl. Inf. Commun. Technol. (AICT)*, Sep. 2017, pp. 1–5.
[15] H. Liang, A. Liu, Y. Zhang, and Q. Zhang, "An ARQ-aided polar coding scheme for security transmission of the wiretap channel," in *Proc. IEEE 2nd Adv. Inf. Technol., Electron. Autom. Control Conf. (IAEAC)*, Mar. 2017, pp. 1530–1535.
[16] N. D. K. Liyanage, C. A. Abeywickrama, P. M. I. U. Kumari, S. A. De Silva, and C. B. Wavegedara, "Performance investigation of hybrid ARQ in HSDPA systems with AMC," in *Proc. Moratuwa Eng. Res. Conf. (MERCon)*, Apr. 2016, pp. 126–131.
[17] M. Y. A. Razak, N. Zainal, and A. R. M. Sidek, "Performance of 8FSK base on PACTOR i protocol over AWGN channels," in *Proc. 5th Int. Conf. Inf. Technol., Comput., Electr. Eng. (ICITACEE)*, Sep. 2018, pp. 152–156.
[18] M. S. Mohammadi, I. B. Collings, and Q. Zhang, "Simple hybrid ARQ schemes based on systematic polar codes for IoT applications," *IEEE Commun. Lett.*, vol. 21, no. 5, pp. 975–978, May 2017.
[19] J. Li and Y. Li, "Modeling ka-band satellite communication system with MPSK," in *Proc. 2nd IEEE Int. Conf. Comput. Commun. (ICCC)*, Oct. 2016, pp. 1785–1789.
[20] A. El Gamal and T. M. Cover, "Multiple user information theory," *Proc. IEEE*, vol. 68, no. 12, pp. 1466–1483, Dec. 1980.
[21] R. Xue, Y. Cao, and T. Wang, "Data-aided and non-data-aided SNR estimators for CPM signals in ka-band satellite communications," *Information*, vol. 8, no. 3, p. 75, Jun. 2017.
[22] Z. Li, D. Yang, H. Wang, N. Wu, and J. Kuang, "Maximum likelihood SNR estimator for coded MAPSK signals in slow fading channels," in *Proc. Int. Conf. Wireless Commun. Signal Process.*, Oct. 2013, pp. 1–6.
[23] E. Matricciani and C. Riva, "Evaluation of the feasibility of satellite systems design in the 10-100 GHZ frequency range," *Int. J. Satell. Commun.*, vol. 16, no. 5, pp. 237–247, Sep. 1998.
[24] C. Loo, "Impairment of digital transmission through a ka band satellite channel due to weather conditions," *Int. J. Satell. Commun.*, vol. 16, no. 3, pp. 137–145, May 1998.
[25] C. Loo, "Statistical models for land mobile and fixed satellite communications at ka band," in *Proc. Veh. Technol. Conf. VTC*, Apr. 1996, pp. 1023–1027.
[26] H. Hussien, K. A. Shehata, M. Khedr, and S. Hareth, "Performance study on implementation of DVB-S2 low density parity check codes on additive white Gaussian noise channel and Rayleigh fading channel," in *Proc. IEEE Int. Conf. Electron. Design, Syst. Appl. (ICEDSA)*, Nov. 2012, pp. 179–182.
[27] J. Huang, Y. Su, W. Liu, and F. Wang, "Adaptive modulation and coding techniques for global navigation satellite system inter-satellite communication based on the channel condition," *IET Commun.*, vol. 10, no. 16, pp. 2091–2095, Nov. 2016.
[28] J. Andrade, N. George, K. Karras, D. Novo, F. Pratas, L. Sousa, P. Ienne, G. Falcao, and V. Silva, "Design space exploration of LDPC decoders using high-level synthesis," *IEEE Access*, vol. 5, pp. 14600–14615, 2017.
[29] X.-Q. Jiang, H. Hai, H.-M. Wang, and M. H. Lee, "Constructing large girth QC protograph LDPC codes based on PSD-PEG algorithm," *IEEE Access*, vol. 5, pp. 13489–13500, 2017.

RUI XUE received the M.S. and Ph.D. degrees in communication engineering and information and communication engineering from Harbin Engineering University, Harbin, China, in 2006 and 2009, respectively. Since July 2003, he has been with the College of Information and Communication Engineering, Harbin Engineering University. From July 2011 to July 2012, he was an Academic Visitor with the Nonlinear Signal Processing Laboratory, The University of Melbourne, Australia. He is currently an Associate Professor with the College of Information and Communication Engineering, Harbin Engineering University. His research interests include the area of radio mobile communication systems, satellite communication systems, and satellite navigation and positioning, and include error-correcting codes, high spectral efficiency modulation, coded modulation, and iterative decoding and detection.

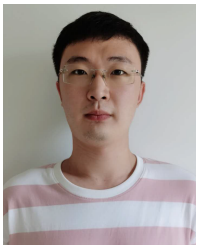

MINGFEI ZHAO received the B.E. degree in communication engineering from Harbin Engineering University, Harbin, China, in 2017, where he is currently pursuing the Ph.D. degree in information and communication engineering. His research interests include satellite communication and satellite navigation, adaptive transmission technology, high spectral efficiency modulation, and spread spectrum communication technology.

HUAIYU TANG received the M.S. degree in radio physics from the China Research Institute of Radiowave Propagation, Xinxiang, China, in 2009. He is currently pursuing the Ph.D. degree in military communications with Xidian University, Xi'an, China. He is also a Senior Engineer with the China Research Institute of Radiowave Propagation. His research interests include the area of the wireless self-organizing monitoring networks, electromagnetic spectrum monitoring, signal recognition, and location technology.